RSC Advances

ROYAL SOCIETY OF CHEMISTRY

www.rsc.org/advances

Trail of Pore shape and Temperature-sensitivity of Poly(N-isopropylacrylamide) Hydrogels before and after Removing Brij-58 Template and Pore Formation Mechanism

Wenjun Gao[a], Qingsong Zhang[a,b*], Pengfei Liu[c], Shuhua Zhang[d], Juan Zhang[a], Li Chen[a]

[a]State Key Laboratory of Hollow Fiber Membrane Materials and Processes, School of Materials Science and Engineering, Tianjin Polytechnic University, Tianjin 300387,China

[b]Department of Chemistry, Tsinghua University, Beijing 100084,China

[c]School of Electronics and Information engineering, Tianjin Polytechnic University, Tianjin 300387,China

[d]Textile Division, Tianjin Polytechnic University, Tianjin 300387,China

* Q.S. Zhang

Corresponding ,author. Tel: +86 022 83955362.

E-mail address: zqs8011@163.com(Qingsong Zhang).

Abstract

To investigate the change upon structure and temperature-sensitivity of porous hydrogel before and after removing template and confirm the pore formation mechanism, a series of hydrogels (abbreviated as CLH) based on *N*-isopropylacrylamide (NIPAM) serving as functional monomer and polyoxyethylene-20-cetyl-ether (Brij-58) acting as template were obtained. The chemical composition, crystal structure and temperature-sensitivity of PNIPAM hydrogels before and after template were compared and confirmed by FTIR, XRD and DSC. The optical performance, pore shape and (de)swelling behavior of prepared CLH hydrogels were investigated by UV/vis, SEM and gravimetric method. The disappearance of characteristic absorption peak at 1062-1146 cm^{-1} and coincidental absorption peak at 195nm, and recovery of diffraction peak at $2\theta = 7.8°$ and $2\theta = 20.75°$ all confirmed that Brij-58 plays a template action and could be removed after 48h. With increasing mass ratios of Brij-58/NIPAM from 0 to 2, the critical time of optical transmittance of CLH hydrogels dropping to 0 from 100 decreases to 7.5 min from 22 min, while maximum equilibrium swelling ratios increase from 6.3 to 10.31g/g. SEM graphs show that, with increasing mass ratios of Brij-58/NIPAM from 0 to 2, CLH hydrogels firstly form homogeneous and smaller pore, and then pore sizes increase from 4-10μm to 50-100μm together with interconnected pore structure. With increasing mass ratios of Brij-58/NIPAM, thermo-responsibility of CLH hydrogels containing Brij-58 template disappeared gradually and then recovered after removing template. The deswelling rates of CLH hydrogels depend on the mass ratios of Brij-58/NIPAM, as r=Brij-58/NIPAM$\leqslant$1/10, the hydrogels lose over 70% water within 60min, while the hydrogel loses over 70% water within 10min as r=Brij-58/NIPAM=2. This kind of templated hydrogel with adjustable porous structure has much potential in the fields of drug delivery system, tissue engineering and chemical separation.

Keywords: hydrogel; N-isopropylacrylamide; Brij-58; template; pore structure

1 Introduction

Porous materials, such as wood, cork, sponges and corals, present widely in our daily life. Interest in the synthesis of porous materials has recently been the focus of extensive research in virtue of widespread application in thermal insulation, filters and purifying systems, bone implants, catalytic substrates, porous battery electrodes, aerators, sorbents, silencers, fiber optics and many others.

As a kind of unique properties of porous material, porous hydrogels formed by polymer networks are capable of retaining or swelling in a large number of water or biological fluids. Due to excellent hydrophilicity, biocompatibility and environmental sensitivity, hydrogels have been served as potential candidates for application in the medical and pharmacological areas.[1-4] Especially, porous hydrogels have been used as scaffolds for tissue engineering applications because of their similarities with extracellular matrix (ECM), excellent biological performance, and inherent cellular interaction capability.

There are many well known methods to prepare porous hydrogel, including phase separation, emulsion-templating synthesis method, porogonic agent, polymer interpenetrating networks and freezing-drying polymerization.[5] The introduction of porous structure would dramatically improve their swelling ability, water absorption rate and stimulation sensitivity. Due to great advantagement in preparing highly porous and well defined macroporous polymers, emulsion-templating method[6-10] has been employed and extensively studied to prepare ordered nano- and macro-porous hydrogel.

Based on such one of emulsion-templating method, free radical or photo-polymerization within liquid crystalline media offers a novel idea to obtain defined porous hydrogel.[11] The hydrogels nanostructure in liquid crystals (LC) serves as a structure directing template, enabling synthesis of polymers with particular structure and properties. Antonietti et al.[12] have successfully prepared porous hydrogels by radical polymerization in lyotropic surfactant phases. The prepared hydrogel presents various morphologies such as “cauliflower” structures, layerlike

architectures, and hydrogel sheets with irregular pores. Additionally, previous studies also have shown that by adjusting the surfactant hydrophobic chain or block copolymer chain segment length to control pore size and shape of hydrogel.[13-15] However, to the best of our knowledge, little work has appeared on the change of structure, pore shape and responsibility before and after template, and also relationship between surfactant concentration and pore morphology although porous hydrogels by polymerization of mixtures containing water and surfactant have been studied. Zhang et al. [16-20] have produced a rapid temperature-sensitive hydrogels by using a non-ionic surfactant, polyoxyethylene-20-cetyl-ether (Brij-58) containing both water soluble (polyoxyethylene) and organic soluble (alkyl chain) segments as template, but there are many questions for waiting to be resolved. Eg. How does the template like Brij-58 work during the polymerization? What's change of chemical structure and properties before and after removing template? What's the relationship between pore size and template concentration?

In this work, Brij-58 with various contents was severed as template to prepare macroporous and temperature-sensitive poly(*N*-isopropylacrylamide) (PNIPAM) hydrogels with pore sizes ranging from 1 to 500 micrometres. The chemical composition and crystal diffraction peak of PNIPAM hydrogels before and after template were compared and confirmed by FTIR and XRD. The thermo-responsibility of PNIPAM hydrogels before and after template was analyzed by DSC. The optical performance, pore shape and (de)swelling behavior of prepared CLH hydrogels were investigated by UV/vis, SEM and gravimetric method. The template mechanism between pore size, shape, distribution and the mass ratios of Brij-58/NIPAM was proposed according to obtained experimental data. The pore size can be accurately controlled by adjusting Brij-58 concentration, and produced porous hydrogel has great application in the field of tissue engineering.

2 Experiments

2.1 Materials

N-isopropylacrylamide (NIPAM, 95%, Tokyo Kasei Kogyo Co.) was purified by twice recrystallization in a mixture of toluene and hexane(60:40, V/V) until formation of spindle-like crystals. Crosslinker *N,N'*-methylenebisacrylamide (MBA, Tianjin Kemiou Chemical Reagent Co.) was purchased by recrystallization in methanol. Nonionic surfactant polyoxyethylene 20 cetyl ether (Brij-58, M_w=1123.5, SERVA Company), HLB (hydrophile-lipophile balance)=15.7, was of analytic grade and was used as received without further purification. Initiator ammonium persulfate (APS) and accelerator *N,N,N',N'*-tetramethylenediamine (TEMED) were purchased from Beifang Tianyi Chemical Reagent and China East Normal University Chemical Factory, Shanghai, respectively. All water used in the whole experiment was of Millipore Milli-Q grade.

2.2 Synthesis of hydrogels templated by Brij-58

Firstly, surfactant Brij-58 with various contents was dissolved in distilled water. Then, 1.5g NIPAM was added to above Brij-58/water system at room temperature under constant stirring and N_2 atmosphere for 30min. The mass ratios of Brij-58/NIPAM in these hydrogel are 0, 1/150, 1/20, 1/10, 1/2, 1, 4/3, 5/3 and 2, respectively. And then 0.1 g MBA was added to the former solution under constant stirring. Thereafter, the initiator 0.01 g APS and accelerator 100 μL TEMED (2% v/v) were added. After 5 min, the generated solutions were poured into 2.0 mm thick glass mold, sealed before placing it and polymerization for 24 h at 24℃. It is noteworthy that when Brij-58/NIPAM is 2, dilute aqueous solution should stir at 40℃ in order to accelerate dissolution of Brij-58.

The resultant hydrogels were taken from glass molds and cut into 1cm discs in diameter with punch, and extensively immersed in deionized water to remove surfactant and other unpolymerized small molecules. Here, the hydrogels thus prepared were labeled as CLH0, CLH001, CLH075, CLH15, CLH75, CLH150, CLH200, CLH250 and CLH300, respectively. The CLH0 means pure PNIPAM hydrogel without any Brij-58. In terms of CLH, C means chemical cross-linked hydrogels, L means the hydrogels using liquid crystal molecule Brij-58 as template, H

means hydrogels.

2.3 Characterization

2.3.1 Maximum Swelling Ratios

The dried CLH hydrogels were weighted (m_d) and immersed in a large amount of deionized water at 25℃ for 48h by changing water several times. Then the CLH samples were taken out and excess water from the surface were removed with filter paper so that the wet weight of swollen CLH hydrogels was measured. The maximum swelling ratios were calculated by following equation[21-22],

$$\text{Maximum Swelling Ratio}(MSR) = \frac{m_e - m_d}{m_d} \quad (1)$$

Where m_e is the weight of CLH hydrogel at equilibrium state and m_d is the dry weight of hydrogel samples, respectively.

2.3.2 UV/vis analysis

The polymerization process of hydrogel pre-reaction solution was in-situ investigated by ultraviolet-visible spectrophotometry (UV/vis, TU-1901, Beijing Purkinje General Instrument Co., Ltd.) with full range scanning to analyze the change of optical performance after the introduction of Brij-58.

To verify template role of Brij-58, CLH hydrogel species were immersed in excessive deionized water at 25℃. The photometric was performed in a given time intervals through UV measurement until it no longer changes.

2.3.3 Fourier transfer infrared spectroscopy

FTIR measurements were carried out using dried CLH hydrogels. The chemical structure of solid samples made from KBr tableting was determined by using a Fourier transform infrared spectroscope (FTIR, TENSOR37, German).

2.3.4 X-ray Diffraction (XRD)

X-ray diffraction (XRD) of freeze-dried CLH hydrogel samples was achieved on Bruker D8 Advance X-ray diffractometer (Germany) with Cu/Kα radiation (λ=1.5406Å), scan speed 2°/min, step 0.02°, 2θ scan range 2.0 ~ 30°.

2.3.5 Scanning electron microscopy (SEM)

The swollen hydrogel discs in deionized water were freeze-dried at -50℃ for 12h on a FD-1A-50 freeze-drier instrument to completely remove any water, and then fractured carefully. The morphologies of the fractured specimens were observed on a Quanta 200 scanning electron microscopy (SEM, FEI Company) at 20kV after sputter coated with gold under vacuum.

2.3.6 Differential scanning calorimeter analysis

About 10mg prepared or swollen hydrogel discs were performed on a differential scanning calorimeter (DSC200F3) under a nitrogen gas atmosphere at a heating rate of 2℃·min^{-1} from 15 to 45℃. Deionized water was used as the reference in the DSC measurement. The volume phase transition temperature (VPTT) was defined as the initial temperature of absorption peak.

2.3.7 Temperature sensitivity analysis

Equilibrium swelling ratios (ESR) of CLH hydrogels at a temperature from 24 to 50℃ were determined in deionized water by gravimetric method and calculated by following equation,

$$ESR = \frac{m_T - m_d}{m_d} \quad (2)$$

Where m_T is the weight of swollen CLH hydrogel under determined temperature, and m_d is the dry weight of CLH hydrogel.

2.3.8 Deswelling Kinetics

The equilibrium CLH hydrogels at 24℃ were put into aqueous water at 37℃. At regular period of time, the CLH hydrogel samples were measured and weighed before returning to the same container. The measurement was performed until there was no further weight decrease. The values of hydrogel water retention (WR) were obtained by following equation,

$$\text{Water Retention}(WR) = \frac{m_t - m_d}{m_e - m_d} \quad (3)$$

Where m_t is the weight of the CLH hydrogel at a given time during deswelling at 37℃, and m_d is the dry weight of hydrogel. When t=0, $m_t = m_e$.

3 Results and Discussion

3.1 Appearance and polymerization process of CLH hydrogels

As a nonionic detergent additive, Brij-58 was selected as a template to blend with monomer NIPAM and cross-linker MBA in the preparation of CLH hydrogel network, Fig.1 shows the appearance of CLH0 and CLH300 hydrogels at swollen and dried state. It is found that the prepared CLH hydrogel samples appear to be milk-white. The reason can be attributed to high cross-linker degree and incorporation of Brij-58. As the mass ratio of MBA /NIPAM is 1/15, the cross-linking position is irregular and network structure is unordered resulting from the difference of chemical reaction rate between MBA and NIPAM. On the other hand, due to the introduction of Brij-58 with various concentrations, the phase separation occurs from micelle-micelle interaction. Hence, the refraction index between water molecules and Brij-58, PNIPAM molecular chain increases, leading to the appearance of milk-white instead of transparency.

To better understand the influence of Brij-58 on optical performance during the polymerization, the polymerization process of CLH hydrogel with various mass ratios of Brij-58/NIPAM has been in-situ examined by UV/vis. Fig.2 shows the optical transmittance spectra of CLH hydrogels as a function of reaction time. It is seen that, with increasing polymerization time from 0 to 30min, the pre-polymerization solution of CLH hydrogel remains around 94% firstly, and then decreases shapely to 0 within 2 min. With increasing mass ratios of Brij-58/NIPAM from 0 to 2, the time of dropping to 0 for CLH hydrogels becomes short. In the case of CLH0 hydrogel, the optical transmittance rapidly drops to 0 at 22 min. It means that, after 22 min, NIPAM free radicals initiated by APS/TEMED and cross-linked by MBA have formed bigger three-dimensional network, leading to great difference in refraction index between hydrogel network and water molecules. Moreover, as 1/2≥Brij-58/NIPAM ≥1/150, the CLH001, CLH075, CLH15 and CLH75 hydrogels with using Brij-58 as template change remain at 13-15min. Especially, as Brij-58/NIPAM≥1.0, CLH150, CLH200, CLH250 and CLH300 hydrogels forming the white opaque sol just need 12.5, 11.5,

10 and 7.5min, respectively. It suggests that the introduction of Brij-58 could rapidly decrease the transmittance of reaction mixture solution. With increasing mass ratios of Brij-58/NIPAM, phase separation occurring from micelle-micelle interaction increases in the same pace, giving rise to rapidly decrease of optical transmittance. Therefore, it is natural that all CLH hydrogels present milk-white after interaction.

3.2 Swelling behavior of CLH hydrogels after template of Brij-58

In the case of the size of CLH hydrogel at swelling equilibrium state, as displayed in Fig.1, the diameters of CLH0 and CLH300 are 1.1cm and 1.3cm, respectively. The increase in sample diameters has initially confirmed that the introduction of Brij-58 can enhance the hydrophilicity of CLH hydrogels. To compare the difference of CLH hydrogels in hydrophilicity/hydrophobicity, maximum equilibrium swelling ratios of CLH hydrogels were obtained (see Figure S1 in the Supporting Information). CLH0 hydrogel exhibits lowest equilibrium swelling ratio, 6.3g/g. And when mass ratios of Brij-58/NIPAM are 1/150, 1/20, 1/10 and 1/2, the maximum equilibrium swelling ratios of CLH001, CLH075, CLH15 and CLH75 hydrogels are 8.30, 7.92, 8.17 and 7.72 g/g, respectively. With increasing mass ratios of Brij-58/NIPAM from 1 to 2, the maximum equilibrium swelling ratios of CLH150, CLH200, CLH250 and CLH300 are 9.05, 9.13, 10.50 and 10.31 g/g, respectively. Then, it can be concluded that the introduction of Brij-58 increases the swelling ratios of pure CLH0 hydrogel.

In general, the swelling equilibrium of hydrogel network depends on the osmotic pressure between polymer chains and water molecules, and restricted by cross-linking degree of balance among network flexibility. In fact, no reaction or cross-linking occurs between Brij-58, NIPAM and MBA. Then it is assumed that Brij-58 plays a key role in increasing maximum equilibrium swelling ratios of CLH hydrogels. On the one hand, the chemical structure of Brij-58 is with hydrophilic group like polyoxyethylene (20). Zhang et al has pointed out that Brij-58 presents highest hydrophilicity in contrast to Brij-52 and Brij-56. On the other hand, it is supposed that Brij-58 serves as a porogenic agent. Depending on the mass ratios of Brij-58/NIPAM,

the pore size and shape are completely different, which would be discussed in section 3.4.

3.3 Chemical composition and structure analysis of CLH hydrogels before and after template

To verify template action of Brij-58, the changes upon chemical structure of CLH hydrogels were first investigated. The FTIR spectra of Brij-58 and the dried CLH001, CLH75 and CLH300 before and after template are shown in Fig.3. It is known to all that NIPAM monomer shows stretching vibration of -C=C- (1622 cm^{-1}), =C-H (917cm^{-1}) and =CH_2 (917cm^{-1}). However, above characteristic absorption peaks of NIPAM don't appear on the spectra curves of CLH hydrogels. It indicates that NIPAM has been polymerized and double bond of -C=C- has been broken into a single bond. As displayed in Fig.3 (A) and (B), the characteristic absorption peak of PNIPAM could also be found, such as C-H stretching vibration at 2972 cm^{-1}, -$(CH_3)_2$ bending vibration at 1387 and 1368cm^{-1}, C=O, N-H, C-N stretching vibration at 1649,1531 and 1456cm^{-1}. For Brij-58, a triple peak appears at 1062-1146 cm^{-1}, which could be attributed to the -CH_2-O-CH_2- stretching vibration. In comparison with Fig.3 (B), Fig.3 (A) shows the triple peak of CLH75 and CLH300 at 1113cm^{-1}, and no clear triple peak presents in the Fig.4 (B). It is speculated that Brij-58 in the CLH hydrogel plays a role of template after immersing into aqueous solution for several days.

To further study the existence formation of Brij-58 in CLH hydrogels matrix before and after template, X-ray diffraction diagrams of CLH hydrogels were shown in Fig. 4. It is seen from Fig. 4 (A) that CLH001 and CLH75 present diffraction peak at 2θ = 7.8° and 2θ = 20.75°, the corresponding *d*-space is 1.10nm and 0.43nm, respectively. However, the diffraction peaks of CLH150 and CLH300 at same position become very weak and almost disappeared, but some faint new diffraction peaks appear. Sun et al[23] has reported that PNIPAM microgel presents a characteristic amorphous diffraction peak at 2θ = 19.7°. Zhang et al[24,25] also thought that PNIPAM microgel/hydrogel shows diffraction peaks at 2θ = 7.74° and 2θ = 21.8°. Therefore, diffraction peak of CLH001 and CLH75 shown in Fig.5 (A) can be ascribed to the

action of PNIPAM like hydrophobic interaction. In the case of Brij-58, there are two obvious diffraction peaks 2θ = 19.4° and 2θ = 23.3°. It is seen that, as the mass ratios of Brij-58/NIPAM≥1, the amorphous diffraction peaks of PNIPAM were covered, while diffraction peaks of Birj-58 manifest. In other words, a small fraction of Brij-58 content has less effect on the diffraction peaks of CLH hydrogel, and diffraction peaks of Birj-58 begin to emerge when mass ratio of Brij-58/NIPAM is bigger than 1. However, it is particularly noteworthy from Fig. 4 (B) that amorphous diffraction peaks of PNIPAM come back after removing Brij-58 template, which suggesting that Brij-58 molecules indeed play a template role. On the other hands, it is also seen that several minor peaks of Brij-58 appear at all CLH hydrogel curves. It indicates that Brij-58 molecules were not removed completely from CLH hydrogel matrix. Then, some removing time is necessary, which will be discussed (see Figure S3 in the Supporting Information).

3.4 Pore structure and shape of CLH hydrogels

Fig.5 shows SEM micrograph of CLH hydrogels after freeze-drying. It is seen that all CLH hydrogels present porous structure with pore size from 5 to 100μm. Since Brij-58 could form micelles in aqueous solution, the original position of Brij-58 was remained after removing template by long soaking, leading to porous structure and various pore sizes. It is found that the pore diameter of CLH0 is approximately 50-70μm with thick pore wall. Compared to CLH0, the pore diameters of CLH001, CLH075, CLH15 and CLH75 have dramatically decreased, only 4-10μm. Interestingly, all pores are interconnected and pore walls are very thinner. In other words, with the introduction of Brij-58, as 1/2≥r=Brij-58/NIPAM>0, CLH hydrogels could form homogeneous and smaller pore. The reason can be ascribed to the formation of micelle. Since critical micelle concentration (CMC) of Brij-58 is 0.077 mmol/L (0.0086%) at 20-25℃, much lower than the concentration of Brij-58 aqueous solution in the experiment, thus congregated Brij-58 molecules form micelle. The polymerization of NIPAM/MBA was performed under the template of micelle, and micro-pore was generated after removing Brij-58 template. It is also particularly

noteworthy that, as 2≥r=Brij-58/NIPAM≥1, the pore diameters of CLH150, CLH200, CLH250 and CLH300 increase sharply to 50-100μm. The reason can be ascribed to the transition of continuous phase and disperse phase. As the mass ratios of Brij-58/NIPAM≥1, phase separation caused by phase inversion occurs, leading to the decrease of porosity and formation of bigger pores. The micrographics of CLH0, CLH75 and CLH250 at different magnifications, as shown in Fig.6, also confirm this tendency. It is found that the pore diameters of CLH0, CLH75 and CLH250 are about 60, 5 and 80μm, respectively. CLH75 presents high compactness because of smallest pore size. Though CLH0 and CLH250 are close in pore size, CLH250 exhibits numerous smaller pores inside of one bigger pore. This kind of composite pore structure with both macro- and micro-pore is the mainly reason that, as the mass ratios of Brij-58/NIPAM≥5/3, CLH250 and CLH300 show highest equilibrium swelling ratios than those of other CLH hydrogels.

As mentioned in Fig.5 and Fig.6, the size and shape of Brij-58 template have close relationship with Brij-58 concentration, and then surface tension of Brij-58 aqueous solution with various concentrations was investigated (see Figure S2 in the supporting information). It can be observed that the surface tension of pure distilled water is 70.5mN/m, while with introducing Brij-58, surface tension dramatically decreases to 39.1mN/m and then keeps approximately at 39mN/m at concentration from 1 to 75g/L. With further increasing Brij-58 concentration from 150 to 200, 250 and 300g/L, surface tension occurs second decrease and becomes 39.2, 35.2, 29.9 and 18.6mN/m, respectively. The rapid decrease of surface tension at beginning can be attributed to decrease of surface free energy of water resulting from the introduction of hydrophilic/hydrophobic Brij-58. The subsequent equilibrium indicates that Brij-58 molecules still manifest as the formation of micelle. With increasing Brij-58 concentration, Brij-58 molecules form hexagonal and cubic phases, leading to continuous decrease of surface tension.

3.5 Thermo-sensitivity and phase transition behavior of CLH hydrogels

The DSC test has been widely used to study the physical and chemical changes

of material. These changes happen in the process of cooling or heating, which present the endothermic and exothermic peak or discrete offset of the baseline on the DSC curves. As is known to all, PNIPAM hydrogel exhibits temperature-sensitivity and presents volume phase transition behavior. Fig.7 shows the DSC curves of CLH hydrogels before and after template.

Fig.7 (A) presents the DSC curves of prepared CLH0, CLH75, CLH15 and CLH300 hydrogels without any purification. It is shown that with the introduction of Brij-58, thermo-responsibility of CLH hydrogels disappeared. It's almost a straight line for CLH300 hydrogel because of excessive amount of Brij-58. In other words, the introduction of Brij-58 into the PNIPAM network has a significant impact on the VPTT value of PNIPAM hydrogel, that is, the decrease of thermo-responsibility. As shown in Figure 7 (A), the green broken line means that the VPTT values of CLH hydrogels before swelling decrease with the increase of mass ratios Brij-58/NIPAM. The reason lies in that aggregated Brij-58 molecules among CLH hydrogel matrix delay or prevent the coil-*to*-globule transition of PNIPAM network upon thermal stimulus.[26,27]

After immersing into aqueous water for longer swelling, the thermo-responsibility of CLH hydrogels resume immediately regardless of Brij-58 content. It can be seen from Fig.7 (B) that all CLH hydrogels curves appear endothermic peak at 32-34℃, which confirming the template action of Brij-58. In particular, as shown in Fig.7 (B), CLH300 shows obvious endothermic peak, completely different with straight line in Fig.7 (A). Moreover, the CLH0 sample in Figure 7 (A) is just prepared without any purification. But, the CLH0 sample in Figure 7 (B) was fully swelled for several days to remove unreacted small molecules or monomer, and the pore size or shape has been changed. As a consequence, DSC peaks of CLH0 in Fig. 7 (A) and (B) are different.

The dramatic changes upon curves tendency between Fig.7 (A) and Fig.7 (B) can be attributed to the role of Brij-58 template. Moreover, there is no any polymerization between Brij-58 and monomer NIPAM, crosslinker MBA. Thus, after template action of Brij-58, the balance of hydrophilic/hydrophobic of CLH hydrogels originating

from amide and isopropyl group recovered, leading to the return of endothermic peak.

Fig.8 shows the dependence of equilibrium swelling ratios of CLH hydrogels upon temperature. With increasing temperature from 24 to 50℃, the swelling ratios decrease 3~10 times, confirming the great thermo-responsibility of CLH hydrogels. Besides, the equilibrium swelling ratios decrease dramatically between 31 and 36℃. The equilibrium swelling ratios of CLH0, CLH001, CLH075, CLH15, CLH75, CLH150, CLH200, CLH250 and CLH300 are 5.83, 4.94, 6.48, 4.11, 6.20, 7.21, 7.05, 8.10 and 8.93 at 31℃, respectively, but have decreased to 1.57, 1.59, 1.38, 1.23, 2.74, 4.80, 6.10 and 7.42 at 36℃, respectively. Therefore, it is reasonable to resume that the VPTT value of CLH hydrogels should be 31-36℃, which is in accordance with the result of Fig.7 (B) determined by DSC. Great changes on swell or shrink behavior around VPTT can be ascribed to the hydrophilic/hydrophobic interactions between water molecules and hydrophilic amide groups (-CONH) or hydrophobic isopropyl groups (-$(CH_3)_3$). At temperature below 31℃, the CLH hydrogel swell on account of hydrogen bonds between water molecules and hydrophilic groups, while when the external temperature exceeds 36℃, the CLH hydrogels present shrinkage state after coil-*to*-globule transition because hydrophobic interactions play a dominant role.

To further analyze the degree of thermo-responsibility of CLH hydrogels around VPTT, the swelling ratio values at 31, 33 and 36℃ were linear fitted. Then the slope values of nine kinds of CLH hydrogel, k, were obtained as follows, -0.85, -0.67, -1.00, -0.58, -0.69, -0.37, -0.45, -0.40 and -0.30, respectively. According to above data, it can be concluded that, different from CLH150, CLH200, CLH250 and CLH300, the rest of hydrogel like CLH0, CLH001, CLH075, CLH15 and CLH75 are strongly influenced by temperature and exhibit excellent thermo-responsibility. In other words, although Brij-58 plays a template role in the process of CLH hydrogel polymerization and thermo-responsibility could recover after template, the introduction of excessive amount of Brij-58, as r=Brij-58/NIPAM $\geqslant$ 1, would fade the temperature-sensitivity of CLH hydrogels. Uncompleted removal of Brij-58 template may be an important reason. The more residual Brij-58 content is, the weaker thermo-responsibility is.

3.6 Deswelling Kinetics

Fig.9 shows the swelling behavior of CLH hydrogels at 37℃. At 37℃ above VPTT of CLH hydrogels, all swollen CLH hydrogels shrink rapidly at initial 40min and then remain stable. Once equilibrium CLH hydrogels were putted into aqueous solution at 37℃, water molecules was leaked out from hydrogel matrix, leading to quickly shrinkage of macroscopic volume and higher water lose rate on account of dominant hydrophobicity. On the other hand, the surface of CLH hydrogels could form a dense layer as the time increase, resulting in slowly release of water molecules from hydrogel matrix. Therefore, the water loss rate no longer changes, and almost remains in a straight line.

It is also noteworthy from Fig.9 that deswelling rate of CLH hydrogels presents close relationship with the mass ratios of Brij-58/NIPAM. According to change tendency of deswelling curves, three parts can be divided. It is found that, as r=Brij-58/NIPAM≤1/10, the hydrogels like CLH0, CLH001, CLH075 and CLH15 lose over 70% water within 60min and reach equilibrium at about 80min. However, as r=Brij-58/NIPAM≥1/2, the CLH hydrogels such as CLH75, CLH150, CLH200 and CLH250 only evacuate less than 50% water within 30min and keep almost the same at remaining 90min. It indicates that, with increasing mass ratios of Brij-58/NIPAM, water molecules could expel out from CLH hydrogel matrix, but at the same time, water loss rate decreases because of formation of dense layer on the surface of CLH hydrogels.[28,29] Interestingly, as r=Brij-58/NIPAM=2, CLH300 hydrogel loses over 70% water within 10min and then has little change. It may be due mainly to the bigger pore size and interconnected pore structure. The water molecules have almost been released before dense layer was formed.

3.7 Template Action of Brij-58 in CLH Hydrogels

To illustrate template action of CLH hydrogels, the UV spectra of Brij-58, CLH0, CLH075 and CLH300 under different removing time are displayed (see Fig. S3 in the supporting information). Here, the removing time means required time that Brij-58 was completely removed from CLH hydrogel by immersing into the aqueous solution.

For Brij-58, an apparent absorption peak occurs at 195 nm. However, for CLH001, CLH75 and CLH300 hydrogels, the absorption peak at 195 nm increases with increasing removing time from 0 to 60 h. It reveals that Brij-58 molecules were gradually removed from CLH hydrogel matrix by immersing into aqueous solution. It is also particularly noteworthy that the two UV/Vis lines of CLH001 and CLH75 at 48 h and 60 h almost coincide with each other, which suggesting that Brij-58 has been basically removed from CLH hydrogel matrix after 48 h.

According to above analysis, it can be drown out that Brij-58 indeed plays a role of template. Although Lu et al[30] and Lester et al[31] have proposed various diagram upon template effect, they are all not real reflect the template action, and only a simple 2D template process was displayed. Here, the schematic diagram of Brij-58 template in the hydrogel matrix was real represented by measured experimental data. According to the mass ratios of Brij-58/NIPAM, three kinds of template mechanisms were proposed, as shown in Fig.10. In pre-polymerization mixture solution, monomer NIPAM, cross-linker MBA, amphiphatic Brij-58, initiator APS and catalyst TEMED distribute randomly. To minimize the system free energy, Brij-58 containing hydrophilic polyoxyethylene and hydrophobic alkyl chain segments (see Fig. S4 in the Supporting Information) will associate each other through hydrophobic interaction and electrostatic force. Thus Brij-58 would form spherical, cylindrical and layered structure under various concentrations on account of differences upon surface tension. During the polymerization, NIPAM, MBA and APS closely distribute around Brij-58, and original state of Brij-58 was remained. After reaction was completed and Brij-58 was removed by immersing into aqueous solution, the original structure occupied by Brij-58 was remained, forming porous hydrogels with controllable pore size and shape. According to SEM results, three kinds of template mechanism were proposed. As 1>r=Brij-58/NIPAM>0, CLH hydrogels form homogeneous and smaller pore ranging from 4-10μm, while as 5/3>r=Brij-58/NIPAM≥1, the pore diameters of CLH hydrogels increase to 50-100μm, and as 2≥r=Brij-58/NIPAM>5/3, composite pore structure with both macro- and micro-pore was formed. The related reason has been mentioned above. Then it is reasonable to conclude that, just by adjusting surfactant

concentration like Brij-58, the hydrogels with pore diameter ranging from 1 to 500 μm or with various shapes like interconnecting pores, macro-pores and nano-micron composite pores could be obtained. This porous structure of hydrogels has much potential in the fields of drug delivery system, tissue engineering and chemical separation.

4 Conclusions

The prepared CLH hydrogels present white because of high cross-linker degree and incorporation of Brij-58. With increasing mass ratios of Brij-58/NIPAM from 0 to 2, the reaction time of optical transmittance of CLH hydrogels dropping to 0 decreases to 7.5 min from 22 min, and maximum equilibrium swelling ratios exhibit an increasing tendency owing to high hydrophilicity and template action of Brij-58. The disappearance of characteristic absorption peak at 1062-1146 cm^{-1} and coincidental absorption peak at 195nm, and recovery of diffraction peak at $2\theta = 7.8°$ and $2\theta = 20.75°$ all confirmed that Brij-58 template was basically removed after 48h. With the introduction of Brij-58, as 1>r=Brij-58/NIPAM>0, CLH hydrogels could form homogeneous and smaller pore, while as 5/3>r=Brij-58/NIPAM≥1, the pore diameters of CLH hydrogels increase sharply to 50-100μm from 4-10μm, and as 2≥ r=Brij-58/NIPAM>5/3, composite pore structure with both macro- and micro-pore was formed. With increasing mass ratios of Brij-58/NIPAM, thermo-responsibility of CLH hydrogels containing Brij-58 template disappeared gradually, but recovered after template action and appear endothermic peak at 32-34℃, and the time reaching deswelling equilibrium decreases. As Brij-58/NIPAM is 2, CLH300 hydrogel loses over 70% water within 10min thanks to the bigger pore size and interconnected pore structure.

Acknowledgements

Great thanks to National Nature Science Foundation of China (21104058, 31200719 & 21174103), and the grant from the Applied Basic Research and Advanced

Technology Programs of Science and Technology Commission Foundation of Tianjin (12JCQNJC01400 & 12JCQNJC08600) for financial support.

References

(1) Aouada, F. A.; De Moura, M. R.; Fernandes, P. R. G.; Rubira, A. F.; Muniz, E. C. *Eur. Polym. J.* **2005**, *41(9)*, 2134-2141.

(2) Tokuyama, H.; Iwama, T. *Langmuir* **2007**, *23*, 13104–13108.

(3) De Moura, M. R.; Aouada, F. A.; Favaro, S. L.;Radovanovic, E.; Rubira, A. F.; Muniz, E. C. *Mater Sci Eng C*. **2009**, *29(8),* 2319-2325.

(4) De Moura, M. R.; Aouada, F. A.; Guilherme, M. R.; Radovanovic, E.; Rubira, A. F.; Muniz, E. C. *Polym test* **2006**, *25(7)*: 961-969.

(5) Yang, J.; Huo, Q. Q.; Hou, C. J. *Mater Rev*. **2010**, *17*,62-65+70.

(6) Tokuyama, H.; Kanehara, A. *Langmuir* **2007**, *23(22)*, 11246.

(7) Imhof, A.; Pine, D. J. *Adv. Mater*. **1998**, *10*, 697-700.

(8) Partap, S.; Rehman, I.; Jones, J. R. *Adv. Mater*. **2006**, *18*, 501-504.

(9) Lua, Y.; Sturekb, M.; Parka, K. *Int. J. Pharm*. **2014**, *461*, 258-269.

(10) Gu, X. Y.; Ning, Y.; Yang, Y.; Wang, C. Y. *RSC advance* **2014**, *4*, 3211-3218.

(11) DePierro, M. A.; Carpenter, K. G.; Allan Guymon, C. *Chem. mater*. **2006**, *18(18)*, 5609-5617.

(12) Antonietti, M.; Caruso, R. A.; Goltner, C. G.; Weissenberger, M.C. *Macromolecules* **1999**, *32(5)*, 1383-1389

(13) Zhang, H. F.; Zhong, H.; Zhang, L. L.; Chen, S. B.; Zhao, Y. J.; Zhu, Y. L.; Wang, J. T. *Carbohyd. Polym*. **2010**, *79(1)*, 131-136.

(14) De Moura, M. R.; Aouada, F. A.; Guilherme, M. R.; Radovanovic, E.; Rubira, A. F.; Muniz, E.C. *Polym. test* **2006**, *25(7)*, 961-969.

(15) Wang, C.; Chen, D.; Jiao, X. *Sci. Technol. Adv. Mat*. **2009**, *10(2)*, 023001.

(16) Zhang, Q. S.; Peng, Z.; Zhang, K.; Chen, L.; Zhao, Y. P. *Acta Polym. Sinica*. **2013**, *(7)*, 841-848

(17) Zhang, Q. S.; Chen, K.; Zhao, Y. P.; Chen, L. *Mater. technol*. **2012**, *27(1)*, 127-129.

(18) Chen, K.; Zhang, Q. S.; Chen, B. J.; Chen, L. *Appl. Clay Sci*. **2012**, *58*,114-119.

(19) Chen, K.; Zhang, Q. S.; Chen, L. *Adv. Mater. Res*. **2011**, *284-286*, 1827-1830

(20)Chen, K.; Chen, L.; Zhang, Q. S.; Wu, B. B. *Acta Phys. Chim. Sin*. **2011**, *27(9)*, 2173-2177.

(21)Pourjavadi, A.; Salimi, H. *Ind. Eng. Chem. Res*. **2008**, 47, 9206–9213

(22)Shang, J.; Shao, Z. Z.; Chen, X. *Biomacromolecules* **2008**, *9*, 1208–1213

(23)Sun, S. T.; Wu, P. Y. *J. Mater. Chem*. **2011**, *21*, 4905-4907.

(24)Zhang, Q. S.; Li, X. W.; Dong, P. P.; Chen, L.; Zhao, Y. P. *Acta Materiae Compositae Sinica*. **2012**, *29(3)*, 105-110.

(25)Zhang, Q. S.; Zha, L. S.; Ma, J. H.; Liang, B. R. *Acta Polym. Sinica.***2007**, *(7)*, 638-643.

(26)Chen, J. Q.; Gong, X. L.; Yang, Hu.; Yao, Y. F.; Xu, M.; Chen, Q.; Cheng, R.S. *Macromolecules* **2011**, *44*, 6227–6231.

(27)Rusu, M.; Wohlrab, S.; Kuckling, D.; Mohwald, H.; Schonhoff, M. *Macromolecules* **2006**, *39*, 7358-7363.

(28)Yui, N.; Mrsny, R. J.; Park, K. *CRC Press LLC*. **2005**.

(29)Wu, Z. G.; Bouklas, N.; Huang, R. *Int. J. Solids Struct.* **2013**, *50*, 578–587.

(30)Lu, C. X.; Du, Z. W.; Li, H. R. *Acta Chim. Sinic.* **2009**, *67(3)*, 238-244.

(31)Lester, C. L.; Smith, S. M.; Colson, C. D. *Chem. mater*. **2003**, *15(17)*, 3376-3384.

Caption of Figures

Fig. 1. Appearance of CLH0 and CLH300 hydrogels before and after removing Brij-58 template.

Fig. 2. The transmittance change of CLH hydrogels pre-polymerization solution within 30min.

Fig. 3. FTIR spectra of Brij-58 and CLH0, CLH75, CLH300 hydrogel before and after removing Brij-58 template.

Fig. 4. XRD patterns of CLH hydrogels before and after removing Brij-58 template.

Fig. 5. SEM images of CLH hydrogel with various mass ratios of Brij-58/NIPAM.

Fig. 6. SEM images of CLH0, CLH75 and CLH250 at three different magnifications.

Fig. 7. DSC thermograms of CLH hydrogel before and after removing Brij-58 template.

Fig. 8. The temperature dependence of equibrium swelling ratios of CLH hydrogels.

Fig. 9. Deswelling behavior of CLH hydrogels at 37℃.

Fig. 10. Pore formation mechanism of CLH hydrogels using Brij-58 as template.

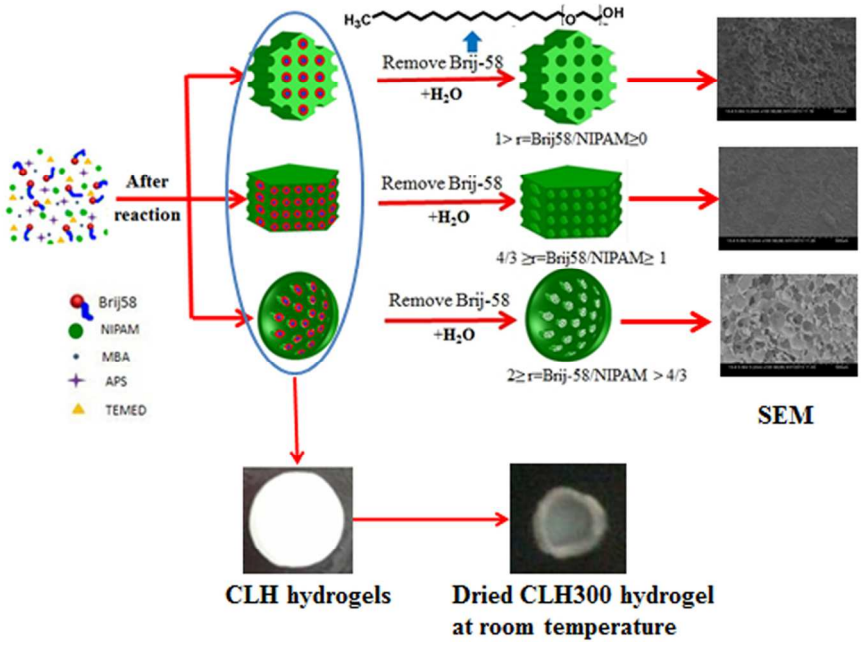

Modulate Porous Morphology and Properties of Thermosensitive Hydrogels by Containing Different Contents of Lyotropic Liquid Crystalline

58x37mm (600 x 600 DPI)

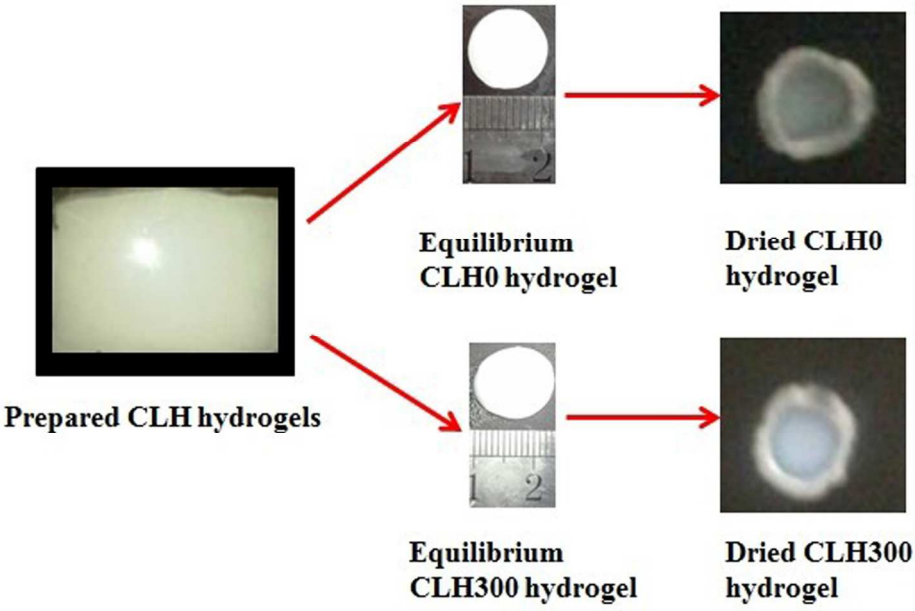

Fig. 1. Appearance of CLH0 and CLH300 hydrogels before and after removing Brij-58 template.
60x40mm (600 x 600 DPI)

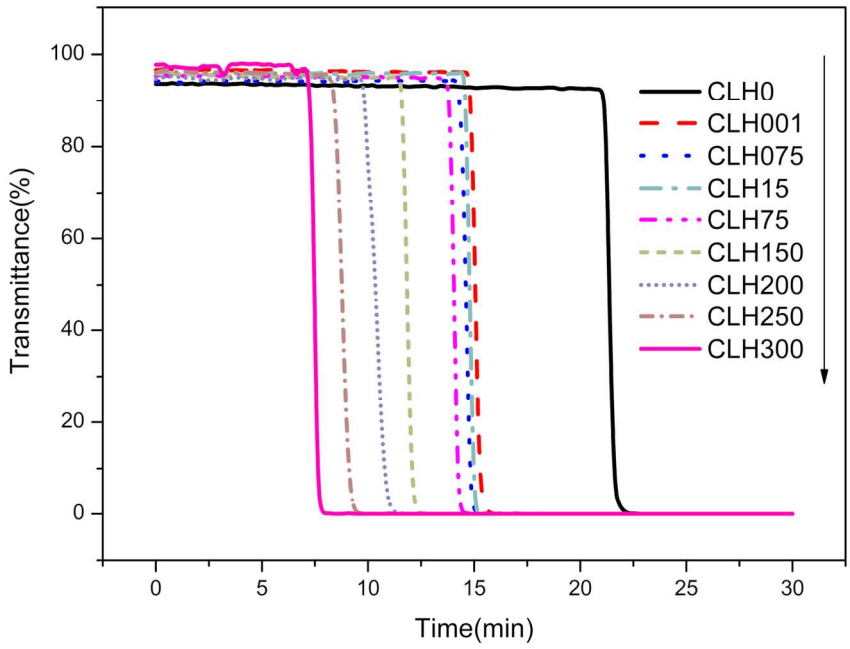

Fig. 2. The transmittance change of CLH hydrogels pre-polymerization solution within 30min.
71x56mm (600 x 600 DPI)

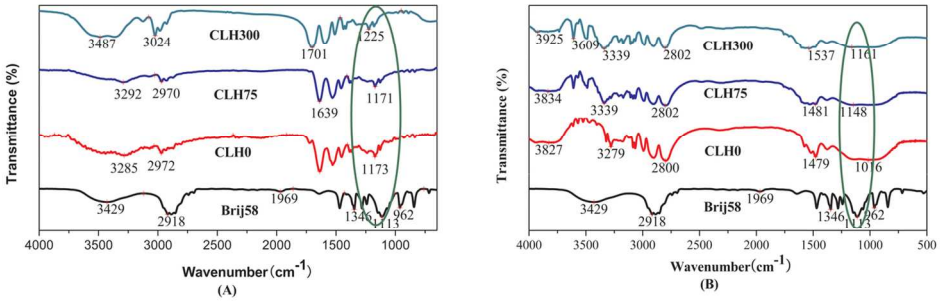

Fig. 3. FTIR spectra of Brij-58 and CLH0, CLH75, CLH300 hydrogel before and after removing Brij-58 template.
63x23mm (600 x 600 DPI)

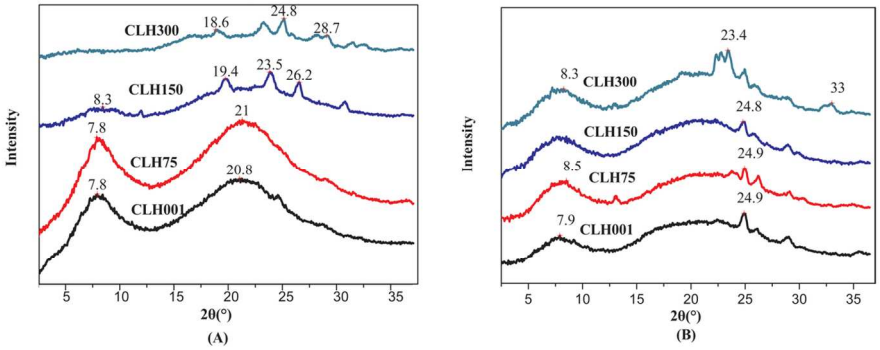

Fig. 4. XRD patterns of CLH hydrogels before and after removing Brij-58 template.
63x22mm (600 x 600 DPI)

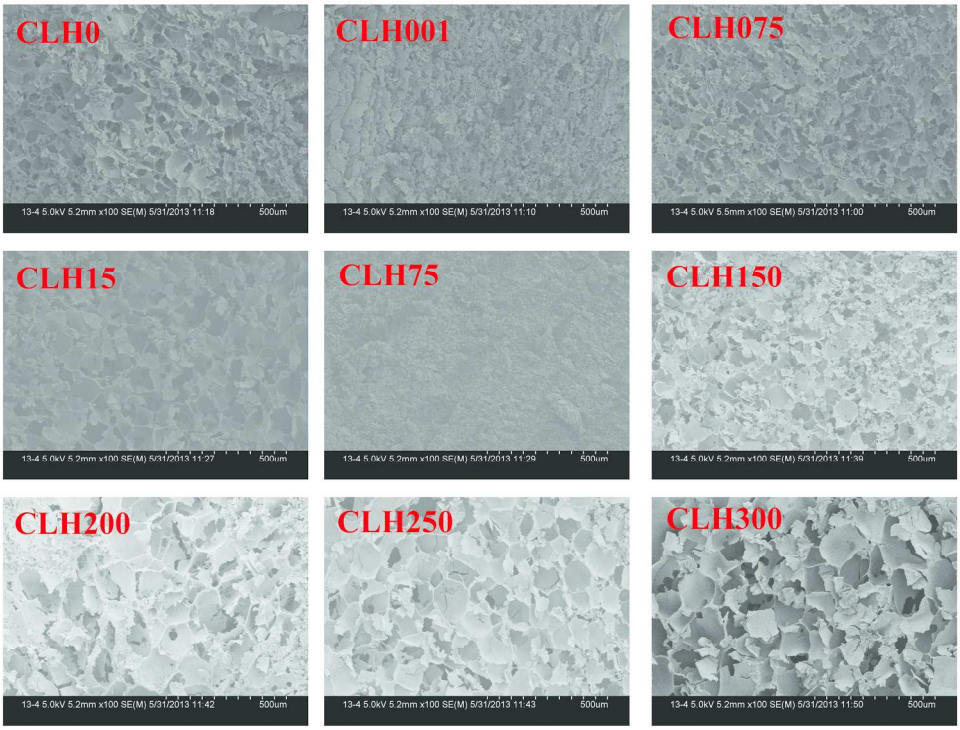

Fig. 5. SEM images of CLH hydrogel with various mass ratios of Brij-58/NIPAM.
266x200mm (300 x 300 DPI)

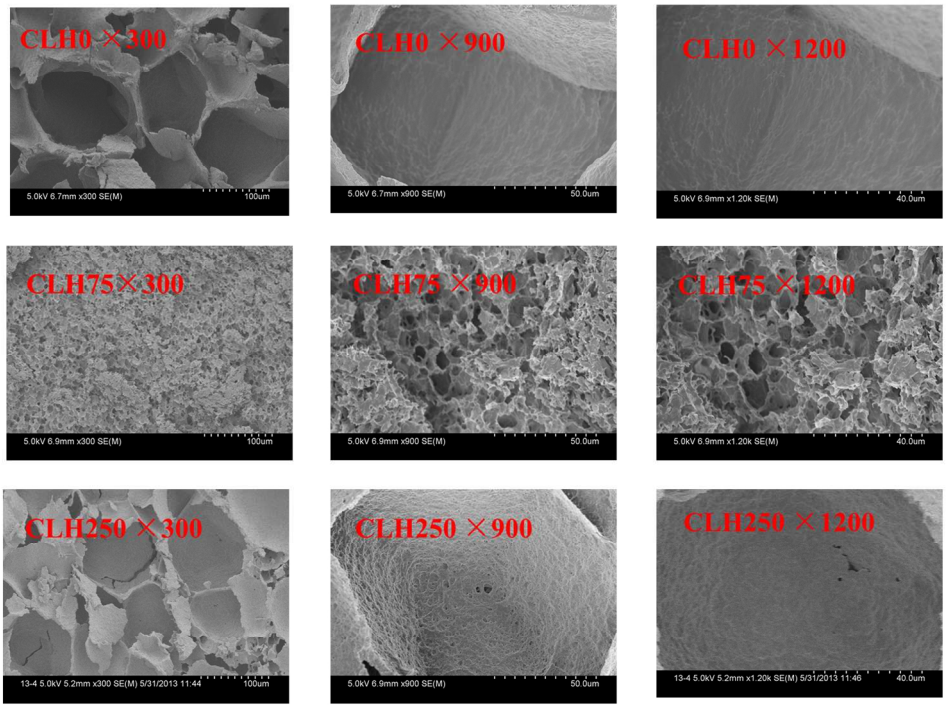

Fig. 6. SEM images of CLH0, CLH75 and CLH250 at three different magnifications.
200x150mm (300 x 300 DPI)

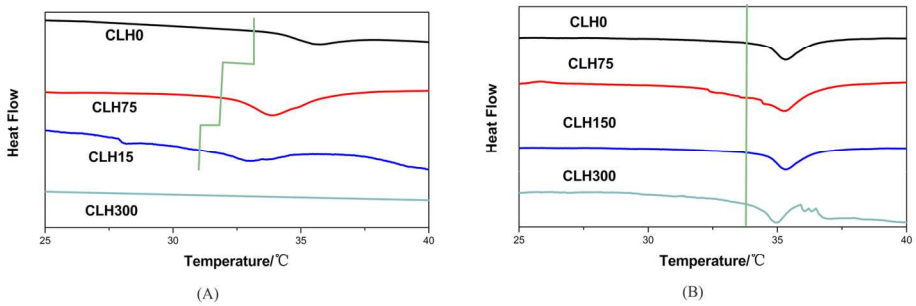

Fig. 7. DSC thermograms of CLH hydrogel before and after removing Brij-58 template.
73x30mm (600 x 600 DPI)

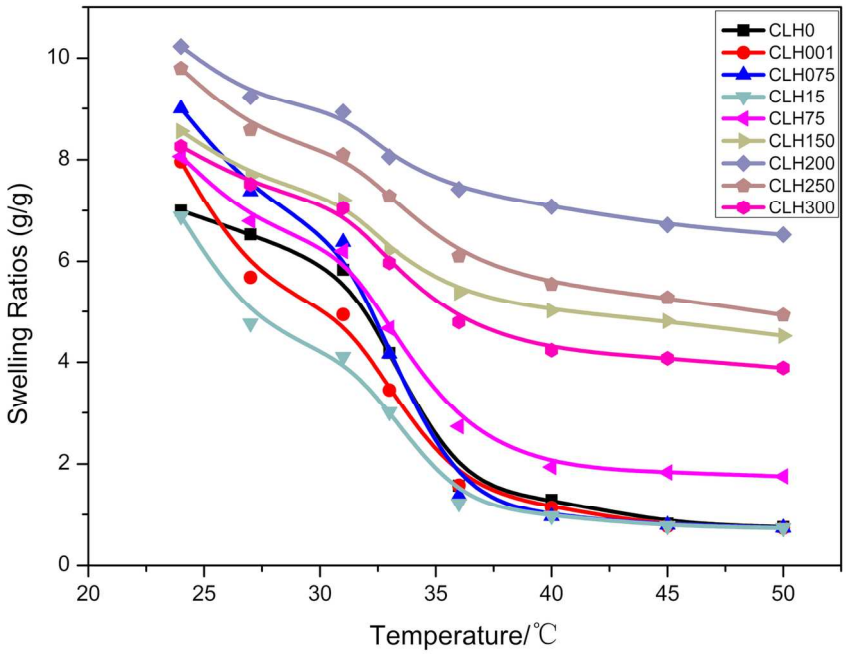

Fig. 8. The temperature dependence of equibrium swelling ratios of CLH hydrogels.
72x58mm (600 x 600 DPI)

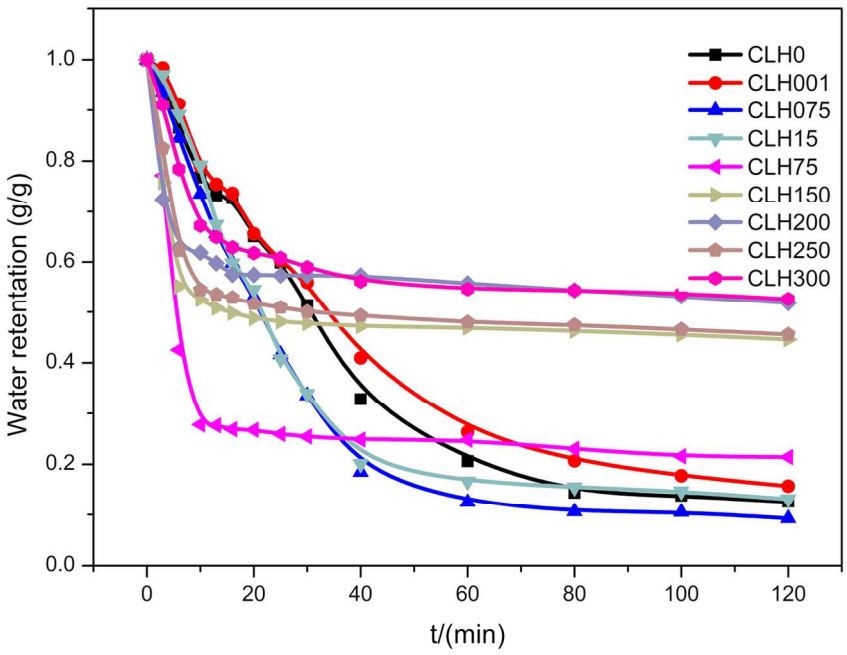

Fig. 9. Deswelling behavior of CLH hydrogels at 37℃.
71x57mm (600 x 600 DPI)

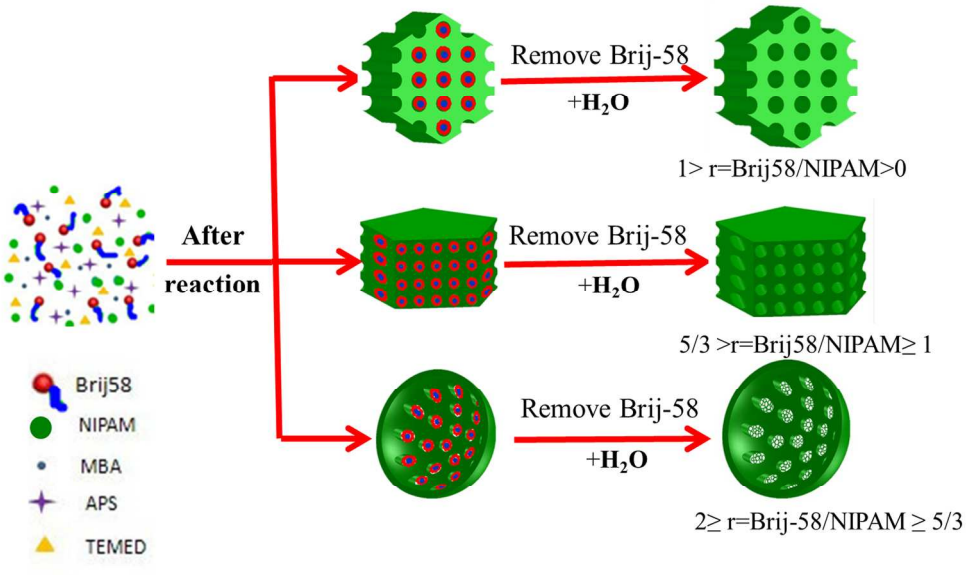

Fig. 10. Pore formation mechanism of CLH hydrogels using Brij-58 as template.
103x60mm (600 x 600 DPI)